Universität Rostock

Traditio et Innovatio

INSTITUT FÜR PHYSIK

Anomalies in Cosmic Ray Composition:
Explanation Based on Mass-to-Charge Ratio

Adrian Hanusch[1], Tatyana Liseykina[1], Mikhail Malkov[2]

Introduction

High precision spectrometry of galactic cosmic rays (CR) has revealed the lack of our understanding of how different CR elements are extracted from the supernova environments to be further accelerated in their shocks. The similarity of He/p, C/p, and O/p rigidity spectra demonstrated by recent AMS-02 measurements has provided new evidence that injection is a mass-to-charge dependent process. Thus, comparing the spectra of accelerated particles with different mass to charge ratios is a powerful tool for studying the physics of particle injection into the diffusive shock acceleration (DSA).

Anomalies in CR composition

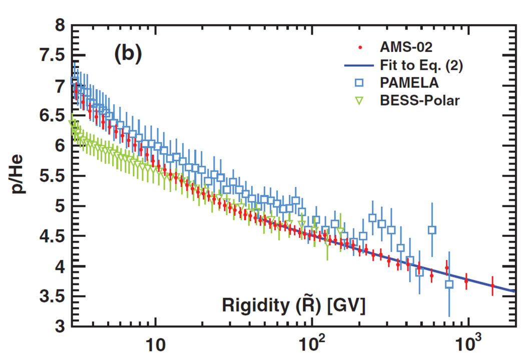

The p/He ratio as a function of particle rigidity. The plot is adopted from [2]

The PAMELA and AMS-02 experiments [1, 2] determined a ≈ 0.1 difference between the rigidity spectral indices of protons and helium. These findings call into question the leading hypothesis CR origin. The CR acceleration mechanism, originally proposed in 1949 by Fermi [3] and actively researched under the name diffusive shock acceleration (DSA), is believed to be electromagnetic in nature. Particles gain energy while being scattered by converging plasma flows upstream and downstream of a supernova remnant (SNR) shock.

From the particle equations of motion in terms of their rigidity $\mathcal{R} = \mathbf{p}\,c/Z\,e$,

$$\frac{1}{c}\frac{d\mathcal{R}}{dt} = \mathbf{E}\,(\mathbf{r},t) + \frac{\mathcal{R}\times\mathbf{B}\,(\mathbf{r},t)}{\sqrt{\mathcal{R}_0^2+\mathcal{R}^2}}, \qquad \frac{1}{c}\frac{d\mathbf{r}}{dt} = \frac{\mathcal{R}}{\sqrt{\mathcal{R}_0^2+\mathcal{R}^2}},$$

it is not difficult to see that even a small, difference in the rigidity spectral indices of different elements may seriously undermine any electromagnetic acceleration mechanism.

Scenarios

1. contribution from several SNRs with different p-He mixtures [4] → not testable
2. spallation [5] → not sufficient for explaining the p/He ratio
3. time-dependence of the shock evolution
   (a) SNR environment [6] → C/He and O/He ratios are independent of $\mathcal{R}$
   (b) time-dependence of shock strength [7] → testable

Assumption

- mass-to-charge dependence of injection
- power law exponent: $q(M) = 4/(1-M^{-2})$
- shock strength (Mach number M) decreases with time
- if He^{2+} is injected more readily at earlier times → harder integrated spectrum

Hybrid Simulation

The dynamics of collisionless shocks can be simulated by means of *hybrid* simulations. In these simulations the ions are treated kinetically,

$$M_i\frac{d\mathbf{v}_i}{dt} = q_i\left(\mathbf{E}+\frac{1}{c}\mathbf{v}_i\times\mathbf{B}-\eta\,\mathbf{J}\right) \quad \text{and} \quad \frac{d\mathbf{x}_i}{dt} = \mathbf{v}_i, \tag{1}$$

while the electrons are assumed to be a massless, charge neutralizing fluid,

$$n_e\,m\frac{d\mathbf{v_e}}{dt} = 0 = -e\,n_e\left(\mathbf{E}+\frac{1}{c}\mathbf{v}_e\times\mathbf{B}\right) - \nabla p_e + e\,n_e\,\eta\,\mathbf{J}, \tag{2}$$

meaning that in this approach the electron scales are neglected. The electron pressure p_e is assumed to be isotropic with an adiabatic relation between pressure and temperature,

$$p_e = n_e\,k_B\,T_e, \qquad \frac{T_e}{T_0} = \left(\frac{n_e}{n_0}\right)^{\gamma-1}, \tag{3}$$

where an adiabatic index of $\gamma = 5/3$ is used. In the Maxwell equations the magnetostatic (Darwin) model is employed,

$$\nabla\times\mathbf{B} = \frac{4\pi}{c}\mathbf{J}. \tag{4}$$

As in usual particle-in-cell simulations, the ion density and current are extrapolated to a grid using a linear weighting, and serve as sources for the calculation of the fields. The electric field,

$$\mathbf{E} = \frac{1}{e\,n}\left(\frac{(\mathbf{J}-\mathbf{J}_i)\times\mathbf{B}}{c} - \nabla p\right) + \eta\,\mathbf{J}, \tag{5}$$

is calculated via a predictor-corrector method and is then used for propagating the magnetic field,

$$\frac{\partial\mathbf{B}}{\partial t} = -c\nabla\times\mathbf{E}. \tag{6}$$

In the simulation dimensionless quantities are used:
t – inverse proton gyrofrequency ω_c^{-1} v – Alfvén velocity v_A
x – proton inertial length c/ω_p n – upstream density n_0
B – upstream magnetic field B_0

The ions are initialized in thermal equilibrium with the electrons with a temperature of $T = mv_A^2/k_B$. In order to model the amount of helium in the interstellar matter a fraction of He^{2+} ions is 10% in number density is added.

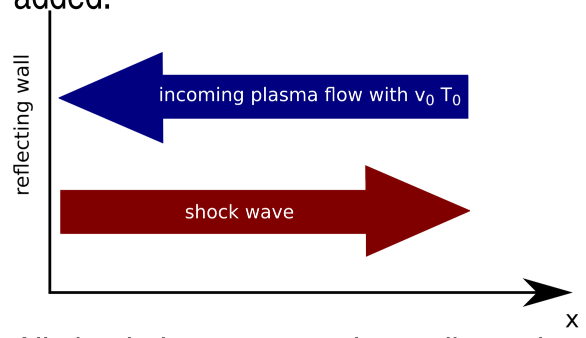

A shock is created by sending a super sonic flow of ions from the right against a reflecting wall. Hence the shock is traveling to the right, parallel to the background magnetic field.

All simulations are quasi one-dimensional (1D spatially, 3D in velocity and fields). The size of the simulation box up to $L_x = 2\cdot10^4\,c/\omega_p$ with a grid spacing of $\Delta x = 0.25\,c/\omega_p$ and 100 particles per cell.

Results

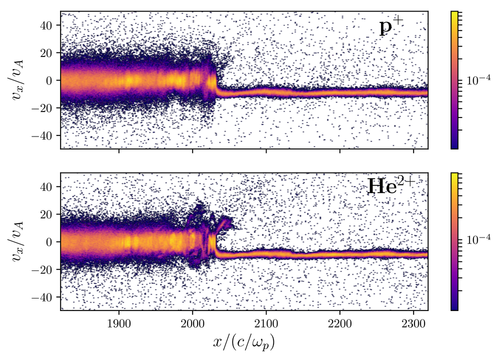

Phase space $f(x, v_x)$ for protons and He^{2+} ions ($v_0 = 10\,v_A, t = 700\,\omega_c^{-1}$). Upstream of the shock transition, the cold inflowing stream is visible. The hot downstream plasma is at rest in the simulation frame.

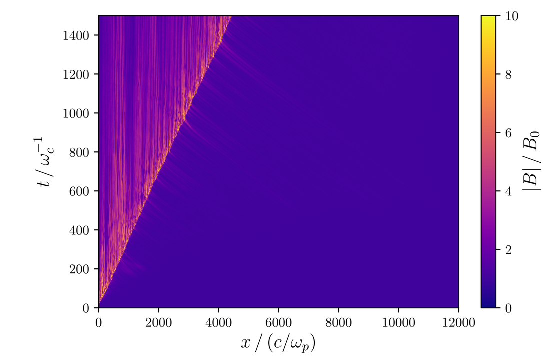

Magnetic field $B(x, t)$ for a simulation with $v_0 = 10\,v_A$. Waves excited by the particles are advected towards the shock and compressed downstream.

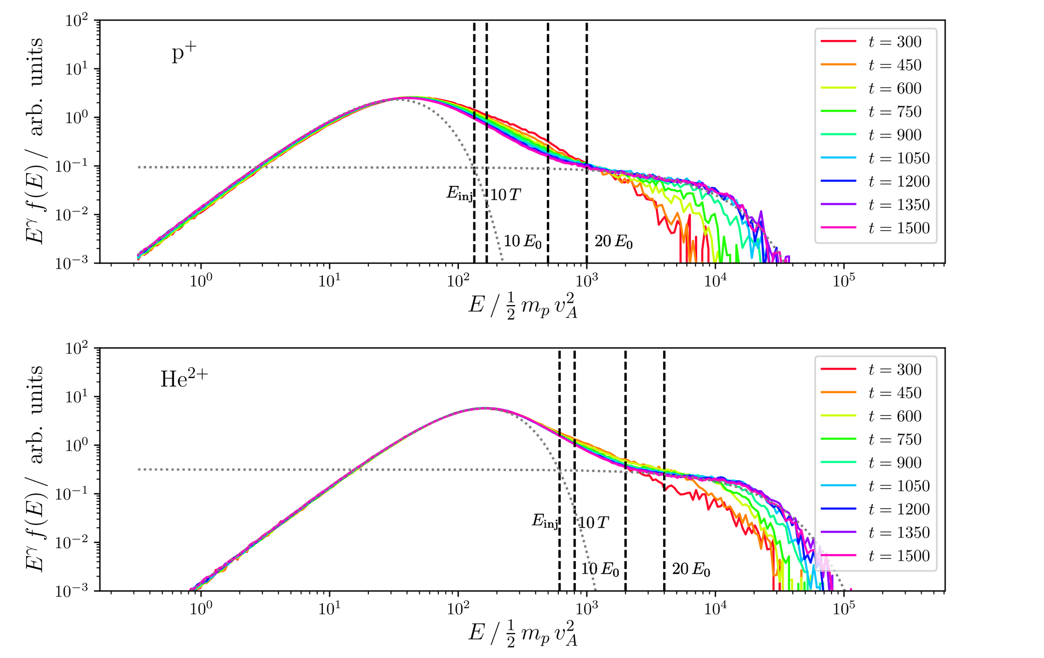

Scaled downstream energy distribution $E^\gamma f(E)$ for as simulation with $M_0 = 10$. The distribution consists of a thermal part and a power-law tail, which develops over time.

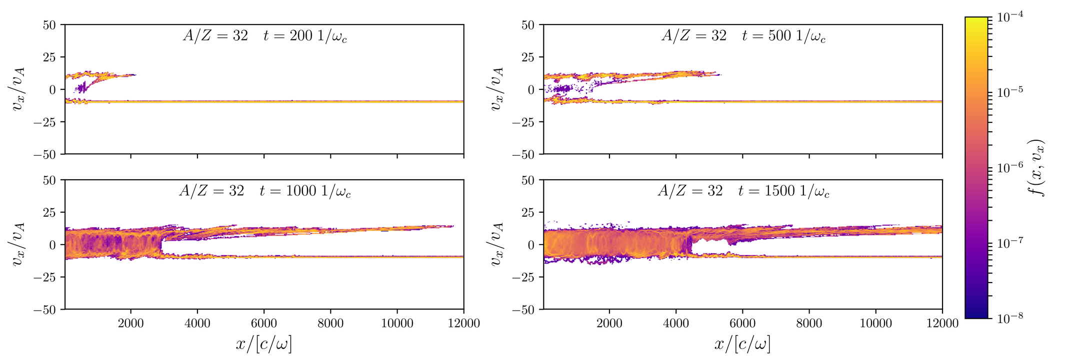

Phase space $f(x, v_x)$ for ions with $A/Z = 32$. In the beginning of the simulation the reflection of the wall is visible. By the end of the simulation the downstream plasma is not thermalized.

Downstream energy spectra ($v_0 = 10\,v_A, t = 1500\,\omega_c^{-1}$) for ions with A/Z up to 32 ($Z = 1$ for all species). For large values of A/Z the particles have not thermalized. Furthermore, the power-law tail is suppressed for the highest mass-to-charge ratio.

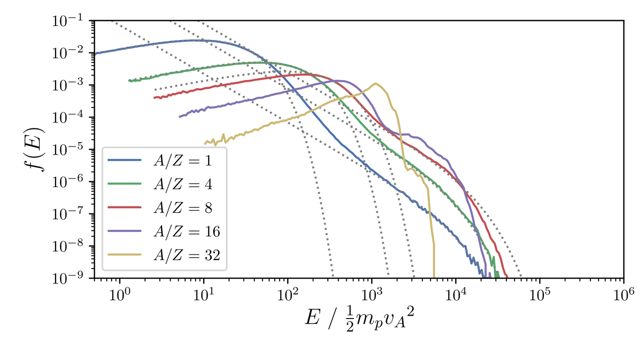

Injection efficiency

The injection energy $E_{\rm inj}$ is calculated from the intersection of the Maxwellian

$$f_{\rm th} = a\sqrt{E}\,\exp(-E/T) \tag{7}$$

and the power-law tail

$$f_{\rm pow} = b\,E^{-\gamma}\,\exp(-E/E_{\rm cut}). \tag{8}$$

The injection efficiency is calculated as

$$\eta_{\rm inj} = \frac{f_{\rm pow}(E_{\rm inj})}{\int_0^\infty f_{\rm th}(E)\,dE}. \tag{9}$$

Injection efficiency η_i obtained from the simulations for different species as functions of the shock Mach number M_s. A simple function of the form $f(M_s) = a(M_s - b)M_s^{-c}$ is fitted to the results. Proton injection is dominant at low Mach number shocks.

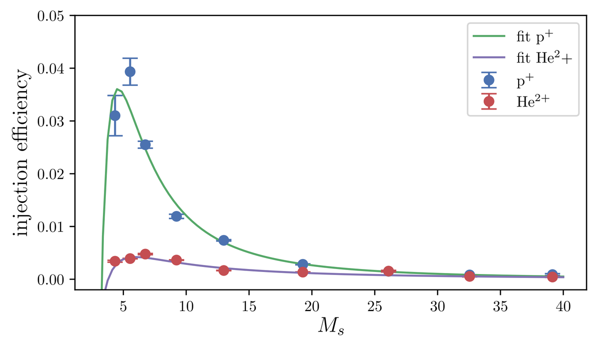

mass-to-charge dependence of the injection

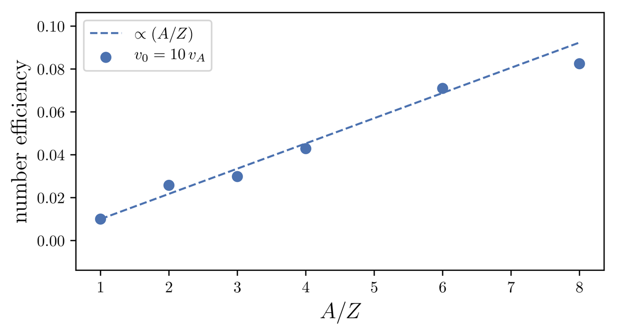

Number efficiency (integral over power-law tail) as function of mass-to-charge ratio A/Z. For small A/Z a linear increase of the injection efficiency with A/Z as in [8] is visible.

p/He ratio

In order to model the time-dependent CR acceleration and extract the p/He ratio, we combine the Mach number dependent injection efficiency with the time dependence of the evolution of a SNR.

Sedov-Taylor phase of the SNR evolution:

$$R_s \simeq C_{\rm ST}\,t^{2/5} \qquad V_s \simeq (2/5)\,C_{\rm ST}\,t^{-3/5} = (2/5)\,C_{\rm ST}^{5/2}\,R_s^{-3/2} \tag{10}$$

with $C_{\rm ST} \simeq (2\,E_e/\rho_0)^{1/5}$, where E_e is the ejecta energy of the supernova and ρ_0 is the ambient density. As the of the shock radius increases from $R_{\rm min}$ to $R_{\rm max}$, the number of CR particles of species α which are deposited in the shock interior can be calculated as

$$N_\alpha(p) \propto \int_{R_{\rm min}}^{R_{\rm max}} f_\alpha(p, M(R))R^2\,dR \propto \int_{M_{\rm max}^{-2}}^{M_{\rm min}^{-2}} f_\alpha(p, M)\,dM^{-2}. \tag{11}$$

Here the spectra are represented in the following way:

$$f_\alpha \propto \eta_\alpha(M)(\mathcal{R}/\mathcal{R}_{\rm inj})^{-q(M)} \qquad \text{with} \quad q(M) = 4/(1-M^{-2}). \tag{12}$$

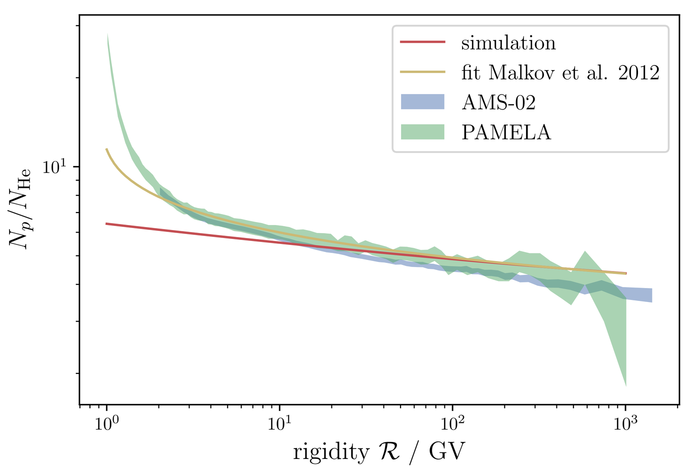

Proton-to-helium ratio as a function of particle rigidity. The results from the simulation (red line) are compared to the PAMELA and AMS-02 data. The observed p/He ratio is accurately reproduced in the range $\mathcal{R} \gtrsim 10$, as expected theoretically.

Acknowledgments

The research was supported by DFG grant TL 2479/2-1, RFBR 16-01-00209, and by NASA ATP-program under grants NNX14AH36G and 80NSSC17K0255. Computational resources provided by the North-German Super-computing Alliance (HLRN) are gratefully acknowledged.

References

[1] O. Adriani, *et al.*, *Science* **332**, 69– April (2011).
[2] M. Aguilar, *et al.*, *Physical Review Letters* **115**(21), 211101 (2015).
[3] E. Fermi, *Physical Review* **75**, 1169–1174 (1949).
[4] V. I. Zatsepin and N. V. Sokolskaya, *Astron. Astrophys.* 458, 5 (2006).
[5] P. Blasi and E. Amato, *J. Cosmol. Astropart. Phys.* 01 (2012).
[6] Y. Ohira, and K. Ioka, *Astrophys. J. Lett.* **729**, L13+ (2011).
[7] M. A. Malkov, P. H. Diamond, and R. Z. Sagdeev, *PRL* **108**(8), 081104 (2012).
[8] D. Caprioli, D. T. Yi, and A. Spitkovsky, *PRL* (2017).

| [1]INSTITUT FÜR PHYSIK - UNIVERSITÄT ROSTOCK | [2]UNIVERSITY OF CALIFORNIA - SAN DIEGO |